Journal of Photochemistry and Photobiology A: Chemistry 217 (2011) 376–382

Contents lists available at ScienceDirect

Journal of Photochemistry and Photobiology A: Chemistry

journal homepage: www.elsevier.com/locate/jphotochem

Utilizing the chemiluminescence of 2-substituted-4,5-di(2-furyl)-1*H*-imidazole–H_2O_2–Cu^{2+} system for the determination of Cu^{2+}

Jing Kang, Yumin Zhang, Lu Han, Jieli Tang, Shuaijun Wang, Yihua Zhang*

College of Chemistry, Jilin University, Changchun 130012, PR China

ARTICLE INFO

Article history:
Received 10 August 2010
Received in revised form 29 October 2010
Accepted 16 November 2010
Available online 21 November 2010

Keywords:
Chemiluminescence
2,4,5-Tri(2-furyl)-1*H*-imidazole
2-phenyl-4,5-di(2-furyl)-1*H*-imidazole
H_2O_2
Cu^{2+}

ABSTRACT

In the paper, 2,4,5-tri(2-furyl)-1*H*-imidazole (TFI) and 2-phenyl-4,5-di(2-furyl)-1*H*-imidazole (PDFI), were chosen to investigate chemiluminescence (CL) properties of 2-substituted-4,5-di(2-furyl)-*1H*-imidazoles. The directly oxidized CL of analytes by H_2O_2 was in detail studied. The H_2O_2 could directly oxidize TFI/PDFI to produce strong CL emission in basic solution. The addition of Cu^{2+} into the system could induce significant enhancement of CL signal. Based on this study, it was found that the TFI/PDFI–H_2O_2–Cu^{2+} CL system could be successfully applied to the determination of Cu^{2+}. The proposed method has been used to determine trace amount of Cu^{2+} with a limit of detection (3σ) of 6.5×10^{-11} mol/L, which enables minimal amount of sample for analysis. A satisfactory result has been obtained for the determination of Cu^{2+} in the reference material samples. The possible oxidized CL mechanism was also discussed briefly based on the photoluminescence (PL) and CL spectra.

1. Introduction

Chemiluminescence (CL) can be defined as emission of light (ultraviolet, visible or infrared) from a molecule or atom in an electronically excited state produced by a chemical reaction at ordinary temperature without any associated generation of heat. There are two types of CL reactions, direct or indirect CL (also described as sensitized or energy transfer CL). Eliminating external light source and employing minimal instrumentation for chemical excitation, CL detection efficiently avoids the factors that limit the sensitivity of classical detections and avoids expensive instrumentation. Owing to its low detection limit, wide dynamic range, rapid response, simple instrumentation and no background scattering light interference, the CL detection method is growing important in analytical chemistry [1–3], particularly in pharmaceutical and biomedical analysis [4–7]. The increase in CL reagents, CL labeling reagents and derivatization methods as well as specific interface designs has widened the application areas of the CL detector.

Over the years, heterocyclic imidazole derivatives have attracted considerable attention because of their unique optical properties [8–10]. These compounds play a very important role in chemistry as mediators for synthetic reactions, primarily as a means for preparing functionalized materials [11]. Imidazole nucleus forms the main structure of some well-known components of human organisms, i.e. the amino acid histidine, vitamin B12, a component of DNA base structure, purines, histamine and biotin. It is also present in structures of many natural or synthetic drug molecules, i.e. azomycin, cimetidine and metronidazole [12]. Phenylimidazoles have been studied because of their important laser properties [13,14]. Further substitution by phenyl groups results in other significant optical properties. An important imidazole derivative is lophine (2,4,5-triphenylimidazole). Recently, a number of lophine derivatives were synthesized based on lophine skeleton substituted at the *ortho*-, *meta*- and *para*-substituted in the 2-phenyl ring and *para*-substituted in the 4- and 5-aryl rings according to slightly modified procedure of the Debus method [15–20]. A variety of lophine analogues having 2-pyridyl or 2-furyl group at both 4- and 5-positions of heterocyclic imidazole derivatives have been reported [19,20]. Among the derivatives, compounds carrying a 2-furyl group showed strong photoluminescence (PL) intensities, while those having a 2-pyridyl group gave very weak intensities [11]. Hitherto, many heterocyclic imidazole derivatives have been synthesized and studied with regard to their ultraviolet (UV), PL and CL properties [18,19]. Lophine is a well-known potential CL compound synthesized by Radziszewski (1877). It has been used for analysis of some metal ions [21–24] and chlorinated compounds [23]. However, application of 2-substituted-4,5-di(2-furyl)-1*H*-imidazoles in CL was quite rare.

* Corresponding author. Tel.: +86 431 85168352 6.
E-mail address: yihuazh47@yahoo.com.cn (Y. Zhang).

1010-6030/$ – see front matter.
doi:10.1016/j.jphotochem.2010.11.009

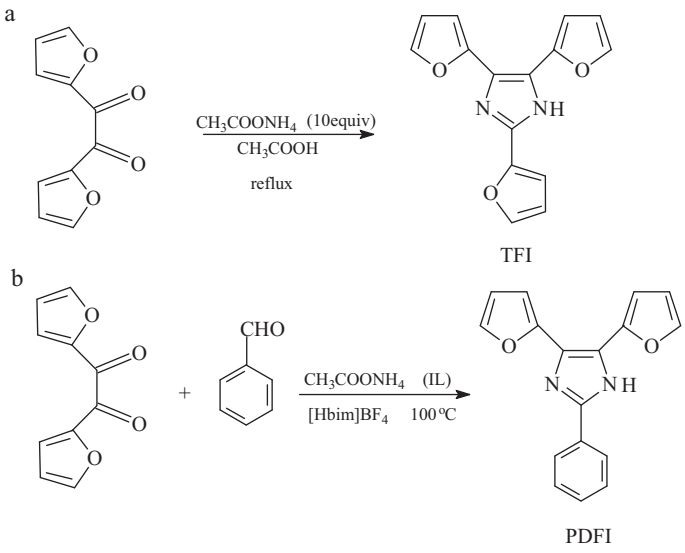

Fig. 1. Synthesis of TFI and PDFI.

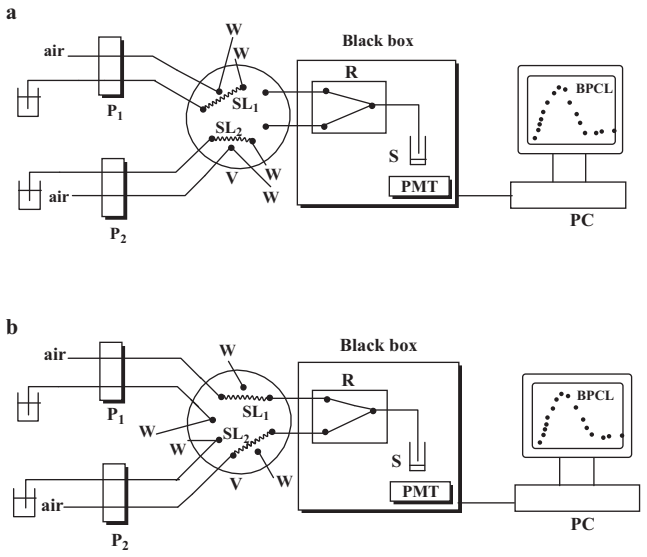

Fig. 2. Schematic diagram of the steady-injection CL system. A: H_2O_2 solution; B: NaOH solution; P_1, P_2: peristaltic pump; SL: sample loop; V: eight-way valve; R: chemifold; S: sample cell; PMT: photomultiplier tube; PC: computer; W: waste. (a) Loading position and (b) injection position.

In the present work, two 2-substituted-4,5-di(2-furyl)-1*H*-imidazoles, 2,4,5-tri(2-furyl)-1*H*-imidazole (TFI) and 2-phenyl-4,5-di(2-furyl)-1*H*-imidazole (PDFI), were synthesized according to the reported methods [20,25]. The H_2O_2 could directly oxidize TFI and PDFI to produce strong CL emission in basic solution. The addition of Cu^{2+} into the TFI/PDFI–H_2O_2 CL systems could induce significant enhancement of CL signal. The possible enhancement mechanism of the CL systems was also further investigated. The proposed method offers the advantages of sensitivity, selectivity, simplicity and rapidity for Cu^{2+} determination. It was successfully applied to the determination of trace amount of Cu^{2+} in the reference materials, such as silicate rock, soil and stream sediments. This may intrigue researchers into gaining a new interest in investigating the CL property of heterocyclic imidazole derivatives.

2. Experimental

2.1. Reagents and chemicals

All the reagents were of analytical reagent grade and all solutions were prepared with double-distilled water. Ammonium acetate, acetic acid, ethyl acetate, methanol, H_2O_2, NaOH, HNO_3, KCl, NaCl, $MgCl_2$, $CaCl_2$, $ZnCl_2$, $Al_2(SO_4)_3{\cdot}18H_2O$, $Ni(NO_3)_2{\cdot}6H_2O$, $BCl_2{\cdot}2H_2O$, $AgNO_3$, $CdCl_2$, $MnSO_4{\cdot}H_2O$, $Cr(NO_3)_3{\cdot}9H_2O$, $Pb(NO_3)_2$, $FeCl_2{\cdot}4H_2O$ and $CuSO_4{\cdot}5H_2O$ were purchased from Beijing Chemical Plant in China. Furfural, petroleum ether and benzaldehyde were purchased from Tianjin Guangfu Fine Chemical Research Institute in China. The certified reference materials such as GSS-4 (limestone soil), GSR-3 (basalt), GSD-2 and GSD-8 (stream sediments) produced by Bulletin of the Institute of Geophysical and Geochemical Exploration (IGGE) in China.

2.2. Synthesis of TFI and PDFI

The synthesis of TFI and PDFI is shown in Fig. 1. TFI was synthesized according to the literature [25]. A mixture of 1 g furil and 4.05 g ammonium acetate in 20 mL acetic acid was heated and refluxed. After completion of the reaction, the mixture was cooled to room temperature, diluted with 100 mL of water, and then neutralized with a 20% NaOH aqueous solution to pH 9. The mixture was extracted with ethyl acetate, and the solvent was removed. The ethyl acetate was evaporated by rotary evaporation. The crude product was further purified by column chromatography using a mixture of petroleum ether and ethyl acetate (3:1) as eluents. Then TFI was recrystallized from methanol. Yellow single crystals were obtained by slow evaporation of the solvent at ambient temperature.

PDFI was synthesized according to the literature [20]. The study was conducted using the ionic liquid (IL), 1-butyl imidazolium tetrafluoroborate ([Hbim]BF_4) as the reaction medium and promoter to generate PDFI by the reaction of furil with benzaldehyde, and ammonium acetate, respectively, at 100 °C. The reaction in the IL was carried out at 100 °C for 24 h. The PDFI was prepared.

2.3. Characterization of TFI and PDFI

The TFI and PDFI were characterized by melting point, IR, MS and NMR. The results obtained by elemental analysis were in conformity with the theoretical results. The results are described as follows.

2.3.1. 2,4,5-Tri(2-furyl)-1H-imidazole (TFI)

M.p. 196–197 °C. IR (KBr) ν (cm^{-1}): 3417, 3114, 2926, 1627, 1538, 1477, 1430, 1380, 1201, 1016, 887, 748. ^{1}H NMR (500 MHz, $CDCl_3$), δ (ppm): 10.48 (s, 1H), 7.42 (s, 2H), 7.36 (s, 1H), 6.92 (d, J = 3.3 Hz, 3H), 6.46 (dd, J = 3.0, 1.7 Hz, 2H), 6.41 (dd, J = 3.1, 1.6 Hz, 1H). MS (m/z): $(M+H)^+$ 267.3 (Calcd. 266.25). Calcd. for $C_{15}H_{10}N_2O_3$: C, 67.65; H, 3.79; N, 10.53. The elemental analysis gave the molecular formula $C_{15}H_{10}N_2O_3$ (Found: C, 67.53; H, 3.71; N, 10.45).

2.3.2. 2-Phenyl-4,5-di(2-furyl)-1H-imidazole (PDFI)

M.p. 197–198 °C. IR (KBr) ν (cm^{-1}): 3118, 3054, 1599, 1551, 1481, 1404, 1233, 1090, 886, 732, 590. ^{1}H NMR (300 MHz, $CDCl_3$), δ (ppm): 7.92 (dd, J = 8.2, 1.5 Hz, 2H), 7.57–7.33 (m, 5H), 6.99 (d, J = 3.3 Hz, 2H), 6.53 (dd, J = 3.4, 1.8 Hz, 2H). MS (m/z): $(M+H)^+$ 277.9 (Calcd. 276.29). Calcd. for $C_{17}H_{12}N_2O_2$: C, 73.80; H, 4.38; N, 10.14. The elemental analysis gave the molecular formula $C_{17}H_{12}N_2O_2$ (Found: C, 73.55; H, 4.34; N, 9.95).

2.4. Apparatus

The CL analysis was conducted on a laboratory-built steady injection CL system. The schematic diagram of the system is shown

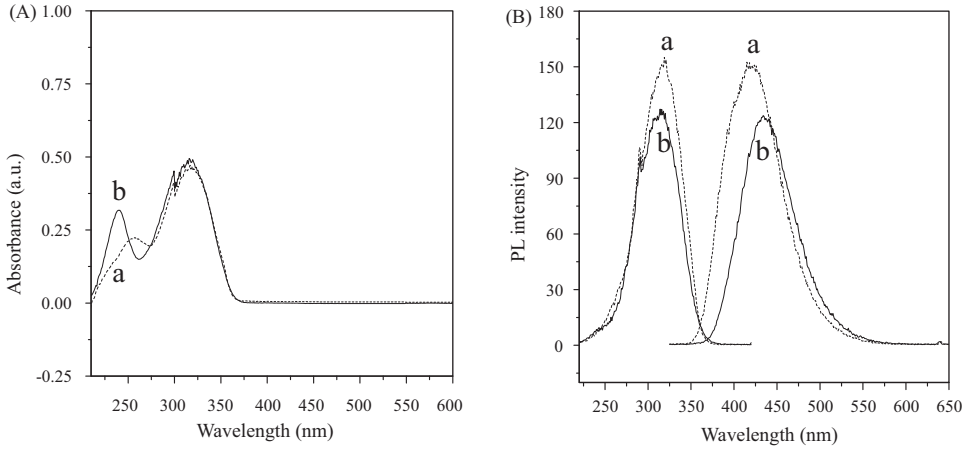

Fig. 3. Absorption spectra (A) and PL spectra (B) of TFI and PDFI. Concentration: TFI (curve a), 2×10^{-6} mol/L; PDFI (curve b), 2×10^{-6} mol/L.

in Fig. 2. The steady injection Analysis Processor FIA-3100 (Beijing Wantuo Instruments Co., Ltd.) consists of two peristaltic pumps, a 16-hole eight-way valve and a digital-system to control the time and pump pressure. PTFE tube (0.8 mm i.d.) was used as connection material in the steady system. The CL emission was detected by an ultra-weak luminescence analyzer (type BPCL manufactured at the Institute of Biophysics, Chinese Academy of Sciences, Beijing, China). The acquisition and treatment of data were performed with BPCL software running under Windows XP.

PL spectra were recorded on a RF-5301 spectrofluorimeter (Shimadzu, Japan). The absorption spectra were recorded on an Australian GBC Cintra 10e UV–vis Spectrometer within the wavelength range from 200 to 800 nm. The CL spectrum was obtained with a series of interference filters. The interference filters were inserted between the sample cell and the PMT. The spectral range detected with the PMT is from 400 to 640 nm.

2.5. Procedure

Experimental results were obtained using the following operation parameters: pump rate, 60 rpm/min; sample loop volume, 300 μL; flow rate, 2.4 mL/min; sampling time, 12 s; sample injection time, 20 s; the PMT negative voltage, −100 V; the integral time of the CL signal, 60 s. 200 μL of TFI/PDFI solution (or solution containing TFI/PDFI and Cu^{2+}) was first added into the sample cell (colorless glass tube 1 cm i.d.), and then H_2O_2 and NaOH solution were synchronously injected into the sample cell using the steady injection system.

In sequence 1 (Fig. 2a), pumps P_1 and P_2 were activated, and valve V was in the loading position. The pump P_1 was used to deliver H_2O_2 solution into the sample loop$_1$ (SL_1) and the pump P_2 was used to introduce NaOH solution into the sample loop$_2$ (SL_2). In sequence 2 (Fig. 2b), pumps P_1 and P_2 were activated, and valve V was in the injection position. The pumps P_1 and P_2 were used to deliver the air current. The H_2O_2 solution and NaOH solution were simultaneously pumped at the same rate separately into chemifold R where they were mixed. The mixed solution was carried into sample cell S and mixed with TFI/PDFI (or solution containing TFI/PDFI and Cu^{2+}) in the sample cell S. CL signal was measured and recorded. After determination, the mixed solution in the sample cell S was emptied. The sample cell S was washed and dried. All experiments were performed in triplicate.

The concentration of analyte was quantified by measuring the change of CL intensity. $\Delta I = I_s - I_0$, where I_0 and I_s are CL signals in the absence and presence of Cu^{2+}, respectively.

2.6. Preparation of sample

0.5000 g of sample was weighed and added to 50 mL beaker. 5 mL of 65% HNO_3 solution was added cautiously into the beaker when the solution was stirred continuously, and slowly heated on the electric hot plate. When there was about 2 mL solution left,

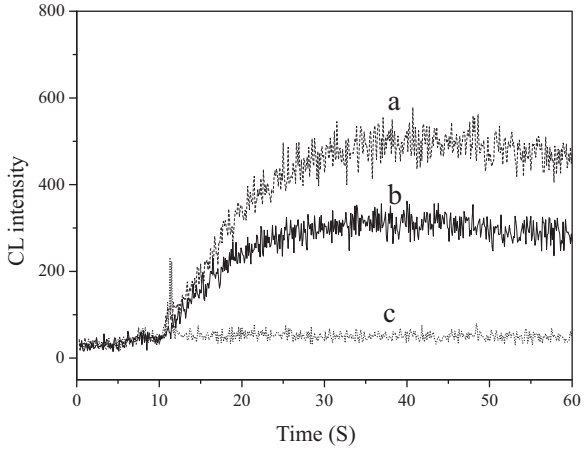

Fig. 4. CL kinetic curves of TFI and PDFI. Concentration: (a) TFI, 0.1 mmol/L; NaOH, 0.1 mol/L; H_2O_2, 1 mol/L, (b) PDFI, 0.1 mmol/L; NaOH, 0.1 mol/L; H_2O_2, 1 mol/L and (c) NaOH, 0.1 mol/L; H_2O_2, 1 mol/L.

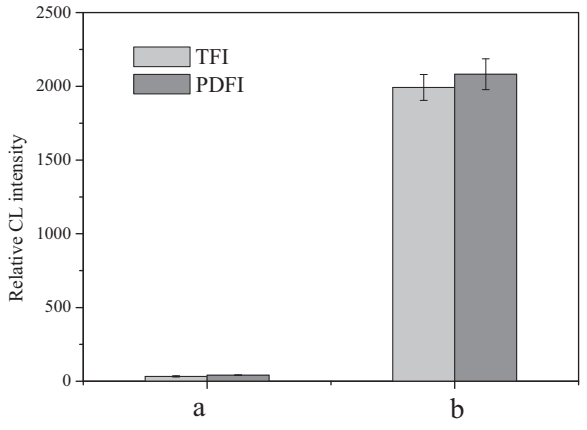

Fig. 5. The catalysis effect of Cu^{2+} on CL intensity. Concentration: (a) TFI/PDFI, 0.1 mmol/L; NaOH, 0.1 mol/L; H_2O_2, 1 mol/L and (b) Cu^{2+}, 0.1 mmol/L; TFI/PDFI, 0.1 mmol/L; NaOH, 0.1 mol/L; H_2O_2, 1 mol/L. The error bars denote the standard deviation of the values with the three same determinations.

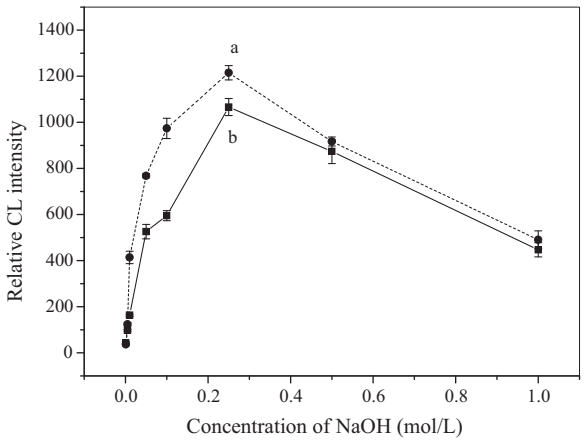

Fig. 6. Influence of NaOH concentration on the CL intensity. Concentration: (a) TFI, 0.1 mmol/L; H_2O_2, 1 mol/L; Cu^{2+}, 0.01 mmol/L and (b) PDFI, 0.1 mmol/L; H_2O_2, 1 mol/L; Cu^{2+}, 0.01 mmol/L. The error bars denote the standard deviation of the values with the three same determinations.

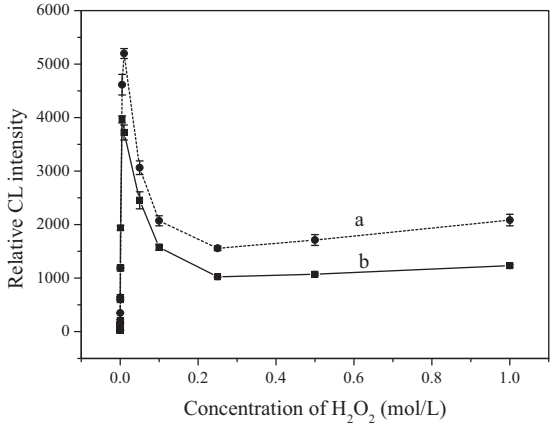

Fig. 7. Influence of H_2O_2 concentration on the CL intensity. Concentration: (a) TFI, 0.1 mmol/L; NaOH, 0.25 mol/L; Cu^{2+}, 0.01 mmol/L and (b) PDFI, 0.1 mmol/L; NaOH, 0.25 mol/L; Cu^{2+}, 0.01 mmol/L. The error bars denote the standard deviation of the values with the three same determinations.

HNO_3 was cautiously added drop-wise for continuous digestion till the HNO_3 are excess. The evaporation was continued until copious reddish brown fumes of nitrogen dioxide are evolved. The residual

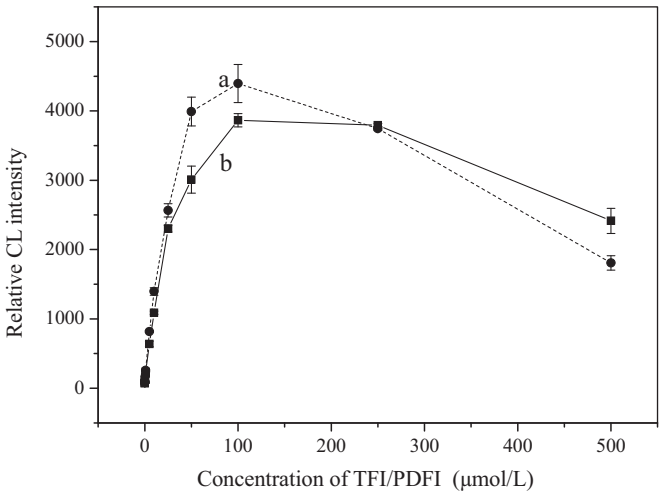

Fig. 8. Influence of TFI/PDFI concentration on the CL intensity. Concentration: (a) H_2O_2, 0.01 mmol/L; 0.25 mol/L; Cu^{2+}, 0.01 mmol/L and (b) H_2O_2, 0.005 mmol/L; NaOH, NaOH, 0.25 mol/L; Cu^{2+}, 0.01 mmol/L. The error bars denote the standard deviation of the values with the three same determinations.

liquid was cooled and proper content of water was added into the beaker. The solution was filtered into the beaker, and the resulting solution was adjusted by NaOH solution to ensure pH value of about 6.5. Then the obtained solution was filtered. The filter liquor was quantitatively transferred into a 250 mL volumetric flask, diluted to the mark at room temperature and mixed thoroughly.

3. Results and discussion

3.1. Absorption spectra, PL spectra and CL kinetic curves of TFI and PDFI

Fig. 3 shows the absorption spectra (Fig. 3A) and PL spectra (Fig. 3B) of TFI and PDFI. It can be seen from Fig. 3A that the first excitonic absorption peaks of the TFI and PDFI appear at 316 and 314 nm, respectively. The PL spectra show that the excitation peaks of TFI and PDFI are at around 319 and 317 nm, respectively, corresponding with the emission peaks of 422 and 435 nm.

The CL reaction between H_2O_2 and TFI/PDFI was further investigated. The H_2O_2 can, in the available concentration range, directly oxidize TFI and PDFI to generate strong CL emission. The dynamic CL intensity-time profiles of the TFI/PDFI–H_2O_2 systems are shown

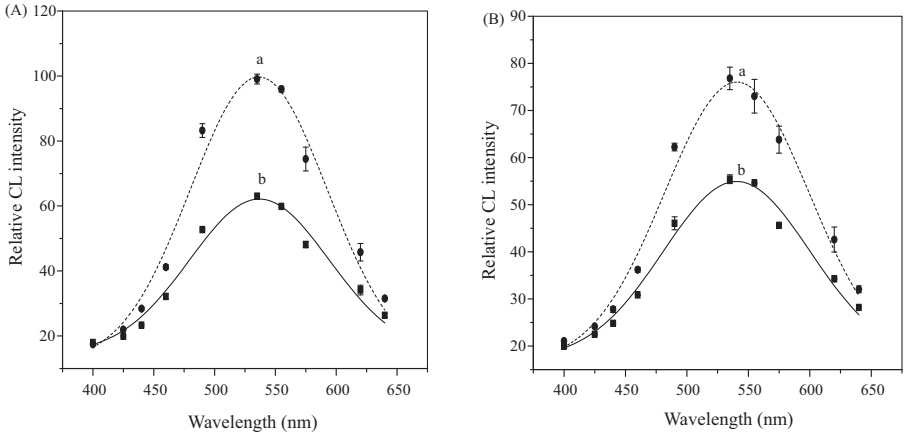

Fig. 9. The CL spectra of different systems. (A) The CL spectra of TFI–H_2O_2–Cu^{2+}system (curve a) and TFI–H_2O_2 system (curve b). Concentration: TFI, 0.1 mmol/L; Cu^{2+}, 5×10^{-7} mol/L; H_2O_2, 0.01 mol/L. (B) The CL spectra of PDFI–H_2O_2–Cu^{2+}system (curve a) and PDFI–H_2O_2 system (curve b). Concentration: PDFI, 0.1 mmol/L; Cu^{2+}, 5×10^{-7} mol/L; H_2O_2, 0.005 mol/L. The error bars denote the standard deviation of the values with the three same determinations.

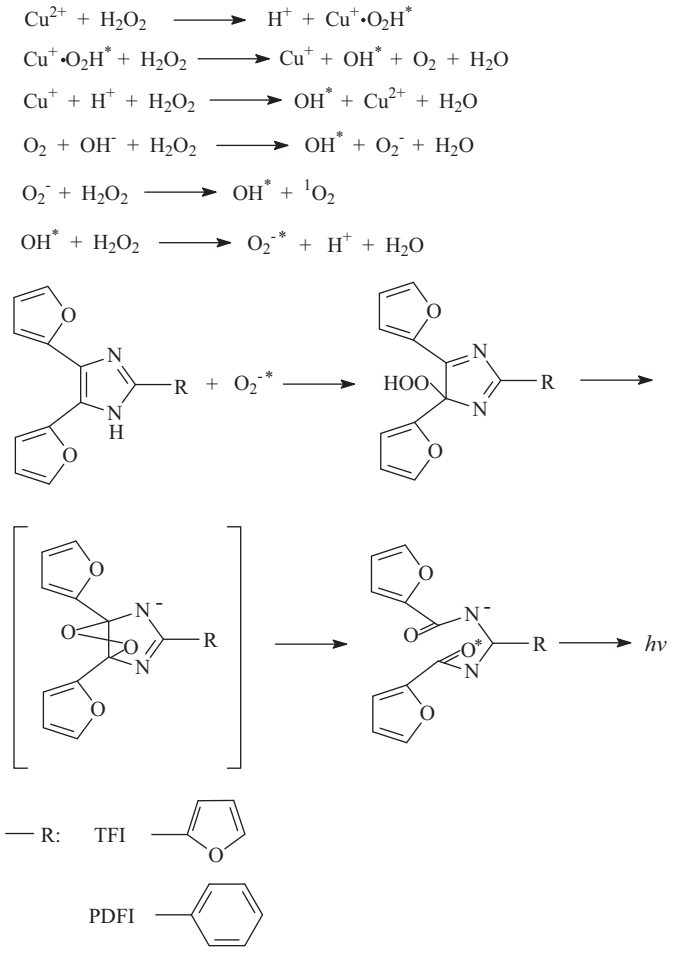

Fig. 10. The mechanism of the CL.

in Fig. 4. It has been found experimentally that the addition of Cu^{2+} into the system could induce significant enhancement of CL signal. The results are shown in Fig. 5. So Cu^{2+} was chosen to enhance the CL intensity of the TFI/PDFI–H_2O_2 system in the experiment.

3.2. Effect of the concentration of NaOH

The effect of the concentration of NaOH on the CL intensity of TFI/PDFI–H_2O_2–Cu^{2+} system was examined in the range of 0.001–1 mol/L, and the results are shown in Fig. 6. The CL intensity increases when the NaOH concentration increases from 0.001 to 0.25 mol/L, and the intensity starts to decrease when the concentration is higher than 0.25 mol/L. Therefore, the optimum NaOH concentration was chosen to be 0.25 mol/L for TFI/PDFI–H_2O_2–Cu^{2+} system.

3.3. Effect of the concentration of H_2O_2

The effect of the H_2O_2 concentration on the CL intensity was studied, and the plot of CL intensity versus H_2O_2 concentration is shown in Fig. 7. From Fig. 7, it can be seen that the CL intensity increases with the increase of the concentration of H_2O_2. The CL intensity reach a maximum when the concentrations of H_2O_2 are 0.01 mol/L and 0.005 mol/L for TFI–H_2O_2–Cu^{2+} and PDFI–H_2O_2–Cu^{2+} system, respectively. When the concentrations of H_2O_2 are higher than 0.01 and 0.005 mol/L for TFI–H_2O_2–Cu^{2+} and PDFI–H_2O_2–Cu^{2+} system, respectively, the CL intensity of the TFI/PDFI–H_2O_2–Cu^{2+} system decreases with the increase of H_2O_2 concentration. So 0.01 and 0.005 mol/L H_2O_2 were chosen for further research, respectively.

3.4. Effect of the concentration of TFI/PDFI

The effect of TFI/PDFI concentration on the CL intensity of the studied system was tested. From Fig. 8, it can be seen that the concentration of the TFI/PDFI has great influence on the CL intensity. With the increase of concentration of TFI/PDFI, the CL intensity increases when the concentration of TFI/PDFI is lower than 0.1 mmol/L, and the intensity decreases when the concentration of TFI/PDFI is higher than 0.1 mmol/L. Therefore, the optimum concentration of TFI/PDFI was chosen to be 0.1 mmol/L.

3.5. Determination of Cu^{2+}

Under the optimal conditions, the relationship between enhanced CL intensity and the concentration of Cu^{2+} was obtained. The analytical parameters are given in Table 1. It demonstrated that there was a good linear relationship between enhanced CL intensity and the concentration of Cu^{2+} over a wide range. The results demonstrate that the analytical figures of merits for the proposed method are satisfactory.

3.6. Selectivity

The interference of some metal ions was tested when the concentration of Cu^{2+} was 5.0×10^{-7} mol/L. The results are listed in Table 2. From the results, it was found that most ions, which generally accompany Cu^{2+}, did not interfere with the detection of Cu^{2+}. The proposed method is quite selective for determination of Cu^{2+}. This fact was further attested by applying the present method to the determination of Cu^{2+} in some samples, including geo-standards of diverse matrices.

3.7. Analytical application

The method finds an excellent application for the determination of Cu^{2+} in the reference materials, such as silicate rock, soil and stream sediments. The results are shown in Table 3. The reference material samples, which were diluted 100-fold, were analyzed. The results obtained were found to be in agreement with the certified values. The relative errors for the analytical results were from −4.0% to 3.1%.

3.8. Study of the mechanism of the system

To explain the CL reaction mechanism and confirm the emission species, the following experiments were performed. The H_2O_2-oxidized CL spectra of TFI/PDFI were measured using a series of high-energy cutoff interference filters, as shown in Fig. 9. It could

Table 1
Linear calibration equation for Cu^{2+}.

System	Linear range (mol/L)	Calibration curve (C, μmol/L)	R	Detection limit (mol/L)	RSD (%)
TFI–H_2O_2–Cu^{2+}	5.0×10^{-10}–1.0×10^{-5}	$\Delta I = 119.7C + 10.92$	0.9972	2.7×10^{-10}	1.8
PDFI–H_2O_2–Cu^{2+}	1.0×10^{-10}–5.0×10^{-6}	$\Delta I = 99.45C + 6.292$	0.9975	6.5×10^{-11}	2.3

The RSD was estimated at 5.0×10^{-7} mol/L for Cu^{2+} ($n = 11$).

Table 2
Tolerance of foreign substances.

Substance	Concentration (μmol/L)	TFI–H_2O_2–Cu^{2+} system change of ΔI (%)	Concentration (μmol/L)	PDFI–H_2O_2–Cu^{2+} system change of ΔI (%)
K^+, Cl^-	500		500	1.0
Na^+, Cl^-	500	−0.7	500	−0.2
Mg^{2+}, Cl^-	10	−2.0	10	−2.0
Ca^{2+}, Cl^-	500	3.1	250	1.2
Zn^{2+}, Cl^-	500	2.0	250	4.5
Al^{3+}, SO_4^{2-}	100	3.7	100	3.1
Ni^{2+}, NO_3^-	50	3.5	5	1.6
Ba^{2+}, Cl^-	500	−0.9	500	−1.7
Ag^+, NO_3^-	25	0.3	25	0.6
Cd^{2+}, Cl^-	10	−2.9	5	3.9
Mn^{2+}, SO_4^{2-}	500	3.0	250	−1.7
Cr^{3+}, NO_3^-	2.5	−1.8	10	−1.4
Pb^{2+}, NO_3^-	10	−2.5	25	−3.4
Fe^{2+}, Cl^-	25	2.8	25	2.7

Concentration of Cu^{2+} is 5.0×10^{-7} mol/L.

Table 3
Determination of Cu^{2+} in diverse samples.

Sample	Certified value (μg/g)	Proposed method (μg/g) ($n = 5$)	Relative error (%)
GSD-2	4.90	4.75 ± 0.08	−3.1
GSD-8	4.10	3.95 ± 0.07	−3.7
GSR-3	48.60	50.11 ± 1.00	3.1
GSS-4	40.00	38.40 ± 0.88	−4.0

be clearly seen from Fig. 9 that there was only one emission band around 460–640 nm for TFI/PDFI–H_2O_2 CL reaction. The CL peaks were at around 535 nm and 540 nm for the TFI–H_2O_2 and the PDFI–H_2O_2 CL reactions, and the corresponding CL spectra are shown in Fig. 9A (curve b) and Fig. 9B (curve b), respectively. The difference of CL peaks for the TFI–H_2O_2 and the PDFI–H_2O_2 system is due to the difference of 2-substituents on the imidazole ring. The PL spectra (Fig. 3B) of the stable emitting species were not identical with the CL spectra. Therefore, it is proposed that the TFI/PDFI can be oxidized to new substance by oxidant. The relaxation of this excited state of the substance induces the transitions, which produces CL signals. The possible oxidized CL mechanism was similar to that of lophine [11,23], and it was clarified that a hydroperoxide as a reaction intermediate is intramolecularly decomposed to yield an excited singlet state of diaroylamidine followed by the emission of light. Fig. 9 also shows significant difference of the CL spectra in the absence and presence of Cu^{2+} for TFI/PDFI–H_2O_2 systems. The CL emission peaks of TFI–H_2O_2 and PDFI–H_2O_2 systems are at about 535 and 540 nm, respectively. When the Cu^{2+} was added into the systems, there was not significant influence on the shapes of the CL emission peaks, but the CL intensity was enhanced. It is suggested that the emission species is excited singlet state of diaroylamidine.

On the basis of many experimental results, the mechanism of the TFI/PDFI CL is proposed to be as follows: (1) Cu^{2+} catalyzes the radical decomposition of H_2O_2 and production of hydroxyl radical (OH*) [26]. (2) In the presence of hydrogen peroxide, the produced hydroxyl radical can be converted into superoxide radical (O_2^{-*}) [27,28]. (3) TFI/PDFI is oxidized by O_2^{-*}; (4) the peroxide excited state diaroylamidines are formed via a dioxetane structure; (5) finally from the excited state, an emission of light occurs. The possible mechanism of CL emission is shown in Fig. 10.

4. Conclusion

TFI/PDFI–H_2O_2–Cu^{2+} CL system was developed in this study. The effect of Cu^{2+} on the TFI/PDFI–H_2O_2 CL system was investigated and the result indicated that Cu^{2+} could effectively enhance the sensitivity of the CL reaction. The effects of experimental conditions were investigated. The increase of CL intensity of the TFI/PDFI–H_2O_2–Cu^{2+} system is proportional to the concentration of Cu^{2+} in the range of certain concentration. Significantly, the method had been used to determine trace amount of Cu^{2+} with a limit of detection (3σ) of 6.5×10^{-11} mol/L. Under the condition of low concentration, the other metal ions (such as Pb^{2+} and Cr^{3+}) do not interfere with the determination of Cu^{2+}. The proposed method is highly selective for determination of Cu^{2+}. The reason may be that Cu^{2+} can catalyze the decomposition of H_2O_2, which can enhance the CL of the TFI/PDFI–H_2O_2 system, and the catalysis reaction is highly selective. The proposed method enables minimal amount of sample for analysis. The lophine CL has been utilized for determination of Cu^{2+} [23], and its major weakness is lack of selectivity. The proposed method has the advantages, such as high sensitivity and selectivity, and wide linear response range. These new phenomena would further enable people to exploit more CL analytical applications of the heterocyclic imidazole derivatives.

References

[1] C.A. Marquette, L.J. Blum, Applications of the luminal chemiluminescent reaction in analytical chemistry, Anal. Bioanal. Chem. 385 (2006) 546–554.
[2] K.A. Fletcher, S.O. Fakayode, M. Lowry, S.A. Tucker, S.L. Neal, I.W. Kimaru, M.E. McCarroll, G. Patonay, P.B. Oldham, O. Rusin, R.M. Strongin, I.M. Warner, Molecular fluorescence, phosphorescence, and chemiluminescence spectrometry, Anal. Chem. 78 (2006) 4047–4068.
[3] M. Tsunoda, K. Imai, Analytical applications of peroxyoxalate chemiluminescence, Anal. Chim. Acta 541 (2005) 13–23.
[4] K. Tsukagoshi, K. Nakahama, R. Nakajima, Direct detection of biomolecules in a capillary electrophoresis–chemiluminescence detection system, Anal. Chem. 76 (2004) 4410–4415.
[5] L. Gámiz-Gracia, A.M. García-Campaña, J.J. Soto-Chinchilla, J.F. Huertas-Pérez, A. González-Casado, Analysis of pesticides by chemiluminescence detection in the liquid phase, Trends Anal. Chem. 24 (2005) 927–942.
[6] J.H. Lin, H.X. Ju, Electrochemical and chemiluminescent immunosensors for tumor markers, Biosens. Bioelectron. 20 (2005) 1461–1470.
[7] J. Yakovleva, R. Davidsson, A. Lobanova, M. Bengtsson, S. Eremin, T. Laurell, J. Emnéus, Microfluidic enzyme immunoassay using silicon microchip with immobilized antibodies and chemiluminescence detection, Anal. Chem. 74 (2002) 2994–3004.
[8] J. Santos, E.A. Mintz, O. Zehnder, C. Bosshard, X.R. Bua, P. Günterb, New class of imidazoles incorporated with thiophenevinyl conjugation pathway for robust nonlinear optical chromophores, Tetrahedron Lett. 42 (2001) 805–808.

[9] N. Fridman, S. Speiser, M. Kaftory, Structures and chromogenic properties of bisimidazole derivatives, Cryst. Growth Des. 6 (2006) 1653–1662.
[10] N. Fridman, S. Speiser, M. Kaftory, Chromotropic behavior of lophine nitro-derivatives, Cryst. Growth Des. 6 (2006) 2281–2288.
[11] K. Nashima, Lophine derivatives as versatile analytical tools, Biomed. Chromatogr. 17 (2003) 83–95.
[12] Ü. Uçucu, N.G. Karaburun, I. Işikdağ, Synthesis, analgesic activity of some 1-benzyl-2-substituted-4,5-diphenyl-1*H*-imidazole derivatives, IL Farmaco 56 (2001) 285–290.
[13] A.C. Testa, Laser flash photolysis study of triphenylimidazole, Spectrochim. Acta, Part A 56 (2000) 901–904.
[14] P. Chou, D. McMorrow, T.J. Aartsma, M. Kasha, The proton-transfer laser. Galn spectrum and amplification of spontaneous emission of 3-hydroxyflavone, J. Phys. Chem. 88 (1984) 4596–4599.
[15] M. Kimura, G.H. Lu, H. Iga, M. Tsunenaga, Z.Q. Zhang, Z.Z. Hu, The stereoselective thermal rearrangement of chiral lophine peroxides, Tetrahedron Lett. 48 (2007) 3109–3113.
[16] N. Fridman, M. Kaftory, S. Speiser, Structures and photophysics of lophine and double lophine derivatives, Sens. Actuators B 126 (2007) 107–115.
[17] K. Nakashima, H. Yamasaki, N. Kuroda, S. Akiyama, Evaluation of lophine derivatives as chemiluminogens by a flow-injection method, Anal. Chim. Acta 303 (1995) 103–107.
[18] N. Fridman, M. Kaftory, Y. Eichen, S. Speiser, Crystal structures and solution spectroscopy of lophine derivatives, J. Mol. Struct. 917 (2009) 101–109.
[19] K. Nakashima, Y. Fukuzaki, R. Nomura, R. Shimoda, Y. Nakamura, N. Kuroda, S. Akiyama, K. Irgum, Fluorescence and chemiluminescence properties of newly developed lophine analogues, Dyes Pigments 38 (1998) 127–136.
[20] S.A. Siddiqui, U.C. Narkhede, S.S. Palimkar, T. Daniel, R.J. Lahoti, K.V. Srinivasan, Room temperature ionic liquid promoted improved and rapid synthesis of 2,4,5-triaryl imidazoles from aryl aldehydes and 1,2-diketones or α-hydroxyketone, Tetrahedron 61 (2005) 3539–3546.
[21] K. Nakashima, H. Yamasaki, R. Shimoda, N. Kuroda, S. Akiyama, W.R.G. Baeyens, Flow-injection analysis of cobalt(II) utilizing enhanced lophine chemiluminescence with hydroxylammonium chloride, Biomed. Chromatogr. 11 (1997) 63–64.
[22] D.F. Marho, J.D. Ingle Jr., Determination of chromium (VI) in water by lophine chemiluminescence, Anal. Chem. 53 (1981) 294–298.
[23] A. MacDonald, K.W. Chan, T.A. Nieman, Lophine chemiluminescence for metal ion determinations, Anal. Chem. 51 (1979) 2077–2082.
[24] D.F. Marho, J.D. Ingle Jr., Ion exchange separation of cobalt from alkaline earth and selected transition metals with lophine chemiluminescence detection, Anal. Chem. 53 (1981) 292–294.
[25] S.J. Wang, Q. Gu, Q. Su, X.D. Chen, Y.M. Zhang, 2,4,5-Tri-2-furyl-1*H*-imidazole, Acta Crystallogr. Sect. E, Struct. Rep. 65 (2009), O3194–U1481.
[26] C.S. Wang, L. Liu, L. Zhang, Y. Peng, F.M. Zhou, Redox reactions of the α-synuclein-Cu^{2+} complex and their effects on neuronal cell viability, Biochemistry 49 (2010) 8134–8142.
[27] Z.P. Wang, J. Li, B. Liu, J.Q. Hu, X. Yao, J.H. Li, Chemiluminescence of CdTe nanocrystals induced by direct chemical oxidation and its size-dependent and surfactant-sensitized effect, J. Phys. Chem. B 109 (2005) 23304–23311.
[28] A.L. Rose, T.D. Waite, Chemiluminescence of luminol in the presence of iron(II) and oxygen: oxidation mechanism and implications for its analytical use, Anal. Chem. 73 (2001) 5909–5920.